Breaking tidal bore: comparison between field data and laboratory experiments

H. CHANSON[a], Y.H. TOI[a]

a. *The University of Queensland, School of Civil Engineering, Brisbane Q4072, Australia*

Résumé :

Un mascaret peut se produire dans une rivière, quand l'embouchure a un fond plat, et une forme convergente, et le marnage est supérieur à 4 à 6 m. Dans cette contribution, on détaille les propriétés des mascarets déferlants et le brassage turbulent induit par ce type de mascaret. En se basant sur une étude de terrain récente [12], et une série d'expérimentations physiques nouvelles, on montre l'effet important du passage du rouleau de déferlement. Une comparaison détaillée est présentée ente les mesures de terrain et de laboratoire, démontrant la validité de la similitude de Froude.

Abstract :

A tidal bore is a surge of waters propagating upstream as the tidal flow turns to rising and the flood tide rushes into a funnel shaped river mouth with shallow waters. The present study focused on the unsteady turbulence induced by a breaking tidal bore through some physical modelling. The laboratory data were compared systematically with some field measurements conducted in the breaking bore of the Sélune River (France) by Mouazé et al. [12]. A key finding was the close agreement in terms of dimensionless free-surface and velocity data between laboratory and field observations. The results supported the implementation of the Froude dynamic similarity.

Mots clefs : Mascaret déferlant, Mesures Physiques, Similitude, Mélange turbulent

Keywords : Breaking tidal bores, Physical modelling, Turbulence, Similarity.

1 Introduction

A tidal bore is a hydraulic jump in translation propagating upstream as the tide turns to rising and the flood flow advances in a funnel-shaped river mouth under spring tide conditions [4]. In France, tidal bores are regularly observed in Aquitaine and in the Bay of Mont Saint Michel (Fig. 1). A tidal bore has a significant impact on the environmental system and the ecology of the river mouth. Recent studies demonstrated in particular the major impact of tidal bores on natural estuarine zones [4, 8, 9]. Surprisingly, many hydrodynamic features remain unexplained and field studies remain limited despite a few successful ones [7, 14, 15, 18].

A bore is a discontinuity of the water depth and it represents a hydrodynamic shock. It is typically characterised in terms of its Froude number. When the bore Froude number is greater than 1.5 to 1.8, a breaking bore is observed with a marked roller. In this study, the unsteady turbulent mixing induced by a breaking bore is detailed based upon new laboratory data. The experimental results are compared with a recent field data set. It is the aim of this study to detail the basic characteristics of the turbulent mixing induced by breaking tidal bores.

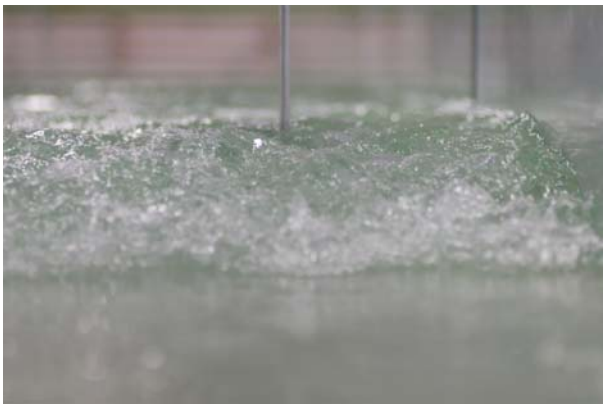

FIG. 1 (Left) - Tidal bore of the Sélune River on 24 September 2010 evening, with bore propagation from right to left - $Fr_1 = 2.35$, $d_1 = 0.375$ m, $B_1 = 35$ m, U = 2 m/s
FIG. 2 (Right) - Laboratory of a breaking bore looking downstream at the incoming bore roller - $Fr_1 = 2.10$, $d_1 = 0.0542$ m, $B_1 = 0.50$ m, U = 0.53 m/s

2 Physical modelling and instrumentation

2.1 Dimensional analysis

An experimental study of tidal bores requires the selection of an adequate similitude. In a dimensional analysis, the relevant parameters encompass the fluid properties and physical constants, the channel geometry, and the initial and boundary conditions [6]. For a tidal bore propagating in a horizontal prismatic channel, a simplified dimensional analysis yields a series of relationships between the dimensionless flow properties at a given location (x, y, z) at time t as functions of a number of relevant dimensionless numbers:

$$\frac{P}{\rho g d_1}, \frac{V_x}{V_1}, \frac{V_y}{V_1}, \frac{V_z}{V_1}, \frac{v_x'}{V_1}, \frac{v_y'}{V_1}, \frac{v_z'}{V_1}, T_{vx}\sqrt{\frac{g}{d_1}}, T_{vy}\sqrt{\frac{g}{d_1}}, T_{vz}\sqrt{\frac{g}{d_1}} = f\left(\frac{x}{d_1}, \frac{y}{d_1}, \frac{z}{d_1}, t\sqrt{\frac{g}{d_1}}, \frac{V_1+U}{\sqrt{g\,d_1}}, \frac{v_1'}{V_1}, \rho\times\frac{(V_1+U)d_1}{\mu}, \frac{B}{d_1}, \frac{g\mu^4}{\rho\sigma^3}, ...\right) \quad (1)$$

where P is the instantaneous pressure, V, v and T_v are respectively the instantaneous mean velocity component, velocity fluctuations and integral time scale, x is the coordinate in the flow direction, y is the horizontal transverse coordinate, z is the vertical coordinate measured from channel bed, the subscript x, y and z refer to the velocity component direction, t is the time, U is the surge celerity, d_1 is the initial depth, V_1 is the initial flow velocity, v_1' is a turbulent velocity fluctuation of the initially steady flow, B is the free-surface width, g is the gravity acceleration, ρ and μ are the water density and dynamic viscosity respectively, and σ is the surface tension between air and water. The right handside term of Equation (1) includes the Froude, Reynolds and Morton numbers, respectively 5th, 7th and 9th terms.

The selection of the Froude similitude follows implicitly from basic theoretical considerations [5, 11]. For the same fluids (air and water) in both model and prototype, the Morton number becomes a constant. In turn, the model Reynolds number is significantly smaller than in the field and viscous scale effects may take place in small size laboratory channels. In the present study, a Froude similitude was adopted and the laboratory results were systematically compared with some field measurements recently conducted in breaking tidal bores [12] to assess potential scale effects.

2.2 Laboratory experiments

The experiments were performed in a 12 m long 0.5 m wide tilting flume previously used by [3]. The channel was made of smooth PVC bed and glass walls. A tainter gate was located at x = 11.15 m where x is the longitudinal distance from the channel upstream end. The tainter gate was a fast closing gate (closing time less than 0.2 s) used to generate a tidal bore propagating upstream against an initially steady flow. The

water discharge was supplied by a constant head tank. It was measured with an orifice meter calibrated in-situ with a V-notch weir system. In steady flows, the flow depth was recorded with a point gauge. The unsteady water depth was measured using acoustic displacement meters Microsonic™ Mic+25/IU/TC, with a dynamic response time of less than 50 ms. The velocity was measured with an acoustic Doppler (ADV) velocimeter Nortek™ Vectrino+. The ADV sampling volume was located at x = 4.5 m. Both the acoustic displacement meters and ADV were sampled simultaneously and synchronously at 200 Hz. The translation of the ADV probe in the vertical direction was controlled by a fine adjustment travelling mechanism connected to a Mitutoyo™ digimatic scale unit.

The experimental setup and flow conditions were selected to generate both breaking and undular breaking tidal bores with the same initial flow rate, although the velocity measurements were conducted in breaking bores only. The main dependant parameter was the tainter gate opening and the flow conditions are summarised in Table 1. Figure 2 illustrates an experiment with a breaking bore.

Table 1 - Turbulent velocity measurements in breaking tidal bores

Reference	Q (m^3/s)	Bed roughness	d_1 (m)	V_1 (m/s)	Fr_1	$\rho\frac{(V_1+U)\,d_1}{\mu}$	Site	Instrumentation
Mouazé et al. [12]	N/A	Mobile bed ('tangue')	0.375 0.325	0.86 0.59	2.35 2.48	1.1×10^6 8.2×10^5	Sélune River (France)	ADV Vector. Sampling: 64 Hz
Present study	0.025	Smooth PVC	0.0517 0.0514 0.0519 0.0508	0.966 0.973 0.963 0.973	2.10 2.02 1.91 1.74	7.7×10^4 7.3×10^4 7.0×10^4 6.2×10^4	Laboratory	ADV Vectrino+. Sampling: 200 Hz

Notes: Q: initial steady flow rate; S_o: bed slope; d_1, V_1: initial flow depth and velocity recorded at sampling location; U: tidal bore celerity positive upstream on the channel centreline; Fr_1: tidal bore Froude number.

3 Basic results

3.1 Flow patterns

The shape of tidal bores is linked with the bore Froude number $Fr_1 = (V_1+U)/(gA_1/B_1)^{1/2}$ where A_1 and B_1 are respectively the initial flow cross-section area and free-surface width. For Froude numbers less than 1.7, an undular bore was seen in the present study. The leading edge of the bore was followed by a train of pseudo-periodic undulations. For Froude numbers greater than 1.7, a breaking bore front was observed (Fig. 2). The bore had a marked roller, or breaking front, extending across the whole width of the channel as seen in Figure 2. The roller size and strength increased with increasing Froude number. A basic flow feature was the roller toe acting as some singularity in terms of air bubble entrainment in the roller and vorticity generation. Both air entrainment and intense turbulent mixing appeared to increase with increasing Froude number. The observations were consistent with earlier findings [1, 3, 8, 9, 16].

The tidal bore flow properties immediately before and after the front must satisfy the continuity and momentum principles [5, 10]. The integral form of mass and momentum conservation gives a series of relations between the flow properties in front of and behind the bore front:

$$\frac{A_2}{A_1}=\frac{1}{2}\left(\sqrt{\left(2-\frac{B'}{B}\right)^2+8\frac{B'/B}{B_1/B}Fr_1^{\,2}}-\left(2-\frac{B'}{B}\right)\right)\frac{B}{B'} \tag{2}$$

where A is the channel cross-sectional area measured perpendicular to the main flow direction, the subscripts 1 and 2 refer to the initial flow conditions and flow conditions immediately after the jump respectively, while B and B' are characteristic widths [5]. For a bore in a rectangular prismatic channel, Equation (2) simplifies into the Bélanger equation:

$$\frac{d_2}{d_1}=\frac{1}{2}\left(\sqrt{1+8\,Fr_1^{\,2}}-1\right) \tag{3}$$

For the present experiments, the ratio of the conjugate cross-sections areas A_2/A_1 at x = 4.5 m are presented as a function of the bore Froude number in Figure 3. The present laboratory data were ensemble-averaged over 25 experiments and they are compared with a range of laboratory and field observations, highlighting a good agreement between laboratory and field data sets.

Some roller free-surface data are shown in Figure 4, where the origin of the horizontal axis is the passage of the roller toe ($t = T_{toe}$). The field and laboratory data showed some time-variations of the bore roller height that were very close to the photographic observations (Fig. 1), as well as to classical longitudinal profiles of breaking hydraulic jumps [2, 13]. The time-variations of the free-surface elevation presented a self-similar profile:

$$\frac{d - d_1}{d_2 - d_1} = \left(\frac{t - T_{toe}}{T_{roller}} \right)^{0.6} \quad (4)$$

where T_{roller} is the duration of the breaking roller. Equation (4) is compared with field and laboratory data in Figure 4 together with the theoretical solution of Valiani [17] for stationary hydraulic jumps.

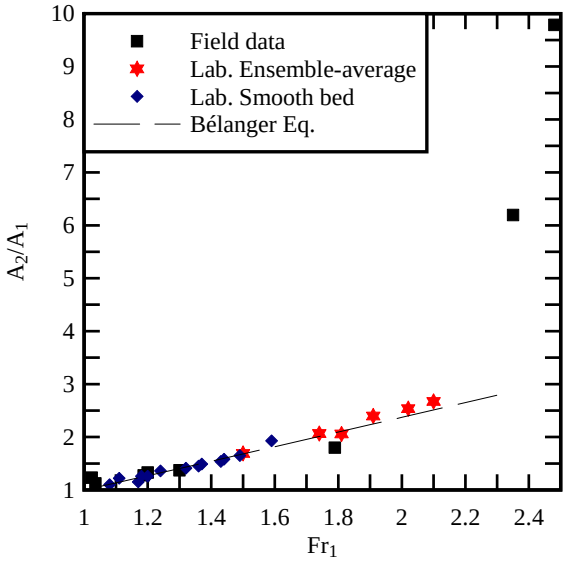

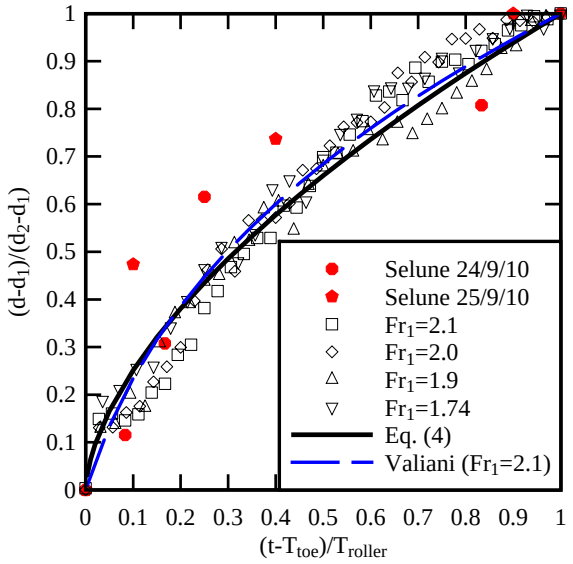

FIG. 3 (Left) - Ratio of conjugate cross-section areas as a function of the Froude number - Comparison between field data [7, 12, 14, 15, 18], laboratory data (Ensemble-averaged: [6], Present study; Single data set: [3, 6] and the Bélanger equation (Eq. (3))

FIG. 4 (Right) - Self-similar free-surface profiles in breaking tidal bores - Comparison between prototype data [12], ensemble-averaged laboratory data (Present study), Equation (4), and the theoretical solution of Valiani [17] for $Fr_1 = 2.1$

3.2 Velocity measurements

The velocity data showed a marked impact of the breaking bore propagation on the velocity field (Fig. 5). Figure 5 present the time-variations of the longitudinal velocity at different vertical elevations during the bore passage, where the longitudinal velocity component V_x is positive downstream towards the river mouth and V_2 is the conjugate flow velocity. The bore passage and sudden rise in the free surface elevation were associated with a sharp flow deceleration. The maximum longitudinal deceleration was 0.14g on average for all laboratory data. For comparison, the field data in the Sélune River gave a maximum deceleration of about 0.16g.

The velocity measurements in laboratory compared favourably with the field data in the Sélune River for a comparable relative elevation z/d_1, as illustrated in Figure 5. The observations were consistent with earlier results in the field [15] and in laboratory [3, 8, 9]. The passage of the breaking bore was associated with some large fluctuations of all three velocity components beneath and behind the bore. A basic flow feature was the occurrence of a transient recirculation next to the invert behind the roller. The transient nature of

the recirculation is linked with the Eulerian measurement technique. The recirculation, highlighted in Figure 5, would follow the bore front. Such a transient recirculation was a feature of breaking bores [3, 9]. The laboratory experiments showed that the amplitude of maximum recirculation velocity decreased with increasing distance from the channel bed. The present data showed that the dimensions of transient recirculation region and the maximum recirculation velocity amplitude increased with increasing Froude number. The maximum recirculation was typically observed shortly after the bore roller in laboratory. The field data in the Sélune River indicated a comparatively longer recirculation zone (Fig. 5), that might be linked with the movable bed and associated changes in bathymetry during the bore propagation.

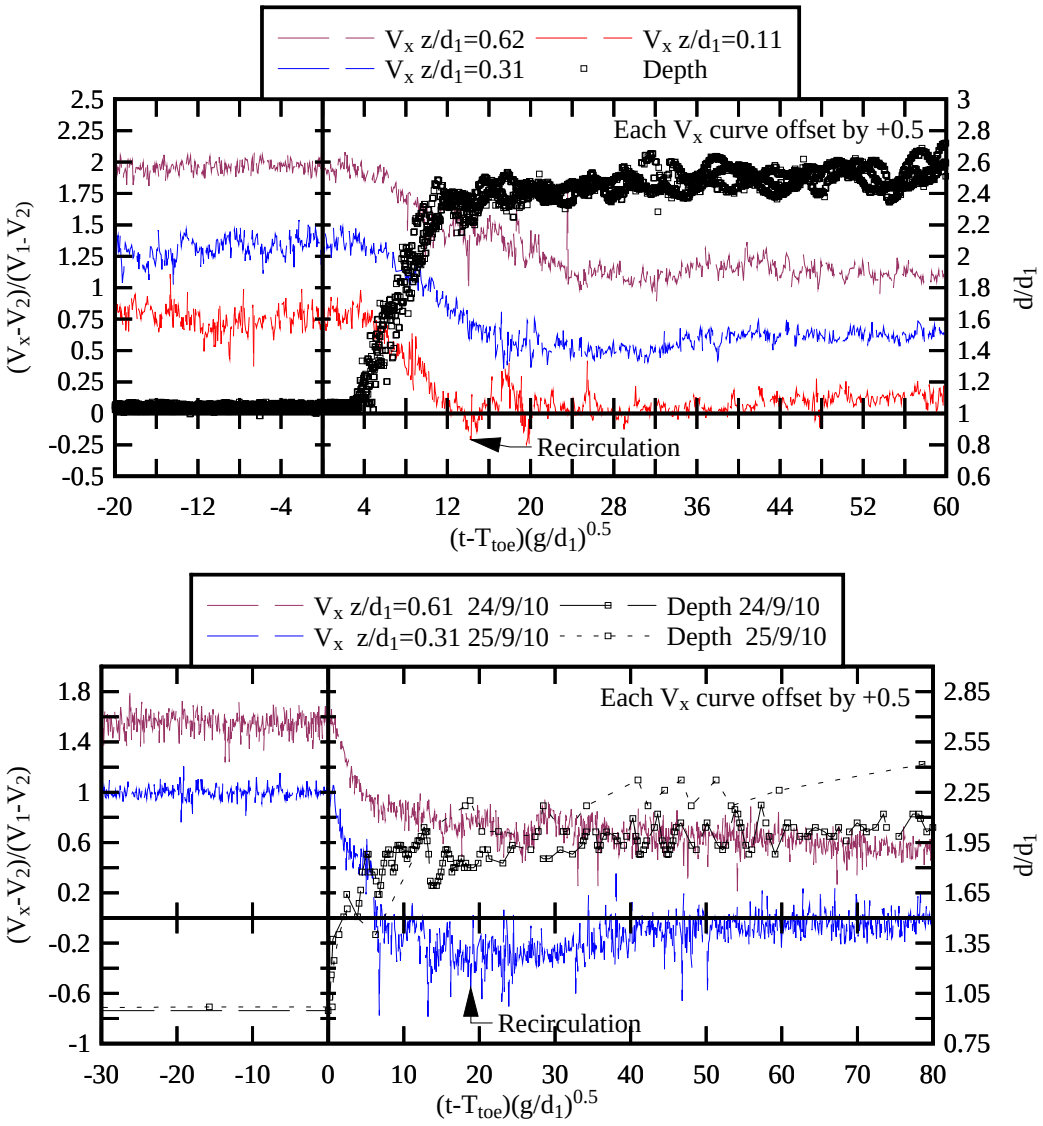

FIG. 5 - Dimensionless water depth and longitudinal velocity measurements in breaking tidal bores: comparison between laboratory (Top, present study $Fr_1 = 2.0$) and field (Bottom, [12]) data - Each longitudinal velocity curve is offset vertically by +0.5 from the previous one

4 Conclusion

The present study investigated the unsteady velocity field induced by breaking tidal bores through some laboratory experiments under controlled flow conditions in a relatively large channel. Detailed free-surface and instantaneous velocity measurements were performed with a high-temporal resolution (200 Hz). The experimental flow conditions were selected to study a range of breaking bores with a minimum number of dependant variables, and the laboratory results were compared with some field measurements conducted in the breaking bore of the Sélune River (France). The propagation of breaking bores was associated with some sharp velocity deceleration at all vertical elevations during the bore passage, followed by some transient

recirculation next to the bed. The roller free-surface profile presented some self-similar relationship similar to classical stationary hydraulic jump observations. An important finding was the close agreement, based upon a Froude similitude, in terms of dimensionless free-surface and instantaneous velocity data between laboratory and field observations, despite some basic differences in initial flow conditions. This has never been tested to that level to date, and the present results supported the physical modelling method first introduced by Koch and Chanson [9].

References

[1] Benet F, and Cunge JA (1971) Analysis of Experiments on Secondary Undulations caused by Surge Waves in Trapezoidal Channels. Jl of Hyd. Res., IAHR, 9(1):11-33.
[2] Chachereau Y, and Chanson H (2011) Free-Surface Fluctuations and Turbulence in Hydraulic Jumps. Experimental Thermal and Fluid Science, Vol. 35, No. 6, pp. 896-909 (DOI: 10.1016/j.expthermflusci.2011.01.009).
[3] Chanson H (2010) Unsteady Turbulence in Tidal Bores: Effects of Bed Roughness. Journal of Waterway, Port, Coastal, and Ocean Engineering, ASCE, 136(5): 247-256 (DOI: 10.1061/(ASCE)WW.1943-5460.0000048).
[4] Chanson H (2011) Tidal Bores, Aegir, Eagre, Mascaret, Pororoca: Theory and Observations. World Scientific, Singapore, 220 pages (ISBN 9789814335416).
[5] Chanson H (2012) Momentum Considerations in Hydraulic Jumps and Bores. Journal of Irrigation and Drainage Engineering, ASCE, 138(4): 382-385 (DOI 10.1061/(ASCE)IR.1943-4774.0000409).
[6] Chanson H, and Docherty NJ (2012) Turbulent Velocity Measurements in Open Channel Bores. European Journal of Mechanics B/Fluids, 32:52-58 (DOI 10.1016/j.euromechflu.2011.10.001).
[7] Chanson H, Reungoat D, Simon B, and Lubin P (2011) High-Frequency Turbulence and Suspended Sediment Concentration Measurements in the Garonne River Tidal Bore. Estuarine Coastal and Shelf Science, 95(2-3): 298-306 (DOI 10.1016/j.ecss.2011.09.012).
[8] Hornung HG, Willert C, and Turner S (1995) The Flow Field Downstream of a Hydraulic Jump. Jl of Fluid Mech., 287:299-316.
[9] Koch C, and Chanson H (2009) Turbulence Measurements in Positive Surges and Bores. Jl of Hyd. Res., IAHR, 47(1):29-40 (DOI: 10.3826/jhr.2009.2954).
[10] Liggett JA (1994) Fluid Mechanics. McGraw-Hill, New York, USA.
[11] Lighthill J (1978) Waves in Fluids. Cambridge University Press, Cambridge, UK, 504 pages.
[12] Mouazé D, Chanson H, and Simon B (2010) Field Measurements in the Tidal Bore of the Sélune River in the Bay of Mont Saint Michel (September 2010). Hydraulic Model Report No. CH81/10, School of Civil Engineering, The University of Queensland, Brisbane, Australia, 72 pages.
[13] Murzyn F, Mouazé D, and Chaplin JR (2007) Air-Water Interface Dynamic and Free Surface Features in Hydraulic Jumps. Jl of Hydraulic Res., IAHR, 45(5):679-685.
[14] Reungoat D, Chanson H., Caplain B. (2012) Field Measurements in the Tidal Bore of the Garonne River at Arcins (June 2012). Hydraulic Model Report No. CH89/12, School of Civil Engineering, The University of Queensland, Brisbane, Australia, 121 pages (ISBN 9781742720616).
[15] Simpson JH, Fisher NR, and Wiles P (2004) Reynolds Stress and TKE Production in an Estuary with a Tidal Bore. Estuarine, Coastal and Shelf Science, Vol. 60, No. 4, pp. 619-627.
[16] Treske A (1994) Undular Bores (Favre-Waves) in Open Channels - Experimental Studies. Jl of Hyd. Res., IAHR, 32(3):355-370.
[17] Valiani A (1997) Linear and Angular Momentum Conservation in Hydraulic Jump. Journal of Hydraulic Research, IAHR, 35(3):323-354.
[18] Wolanski E, Williams D, Spagnol S, and Chanson H (2004) Undular Tidal Bore Dynamics in the Daly Estuary, Northern Australia. Estuarine, Coastal and Shelf Science, Vol. 60, No. 4, pp. 629-636.